https://doi.org/10.1177/0954406219861126

Inverse procedure for mechanical characterization of multi-layered non-rigid composites parts with applications to the assembly process

Ngoc-Hung Vu[1], Xuan-Tan Pham[1*], Vincent François[2] and Jean-Christophe Cuillière[2]

Abstract

In assembly process, non-rigid parts in free-state may have different shapes compared to the designed model due to geometric variations, gravity load and residual stresses. For non-rigid parts made by multi layered fiber-reinforced thermoplastic composites, the assembly process becomes much more complex due to the nonlinear behavior of the material. This paper presented an inverse procedure for characterizing large anisotropic deformation behavior of four-layered, carbon fiber reinforced polyphenylene sulphide, non-rigid composites parts. Mechanical responses were measured from the standard three points bending test and the surface displacements of composite plates under flexural loading test. An orthotropic hyperelastic material model was implemented in the user-defined material subroutine of Abaqus for finite strain shell elements to analyze the behavior of flexible fiber-reinforced thermoplastic composites. Error functions were defined by subtracting the experimental data from the numerical mechanical responses. Minimizing the error functions helps to identify the material parameters. These material parameters were validated for the case of an eight-layered composite material.

Keywords: Finite element method; Finite strain shell element; Anisotropic material model; Fiber-reinforced composites; Assembly process.

1. Introduction

One important element in the quality control of products is to analyze whether the post-assembly shape fulfills the designer's geometric specifications. This task is performed by evaluating the component's shape after having mounted it into the final assembled configuration. Large non-rigid parts in *free-state*, such as aerospace panels may have deviations from their nominal (CAD) shape caused by geometric variations, gravity load and residual stresses. It makes the assembly process difficult, even impossible when the deviation is out of tolerance. To solve this problem, a non-rigid part must be mounted on special fixtures to simulate the *assembly-state*. Then, the mismatches between its real geometry and its target nominal geometry are evaluated. This process is usually carried out by using coordinate measuring systems or laser scanners. Figure 1 shows an example of an aerospace panel restrained by known forces (weight) on its inspection fixture before the measurement process. This inspection task is generally laborious and time-consuming. Therefore, there is a great interest in the industry towards developing virtual inspection methods, which can significantly reduce inspection time and cost.

Figure 1. An aerospace panel restrained by known forces on its inspection fixture [1]

Some researchers [2-5] proposed virtual inspection methods based on numerical approaches by building a finite element (FE) model of the non-rigid part considerd in free-state. Boundary conditions were then imposed on this FE model to constrain the part to its working shape. The virtual restrained part was compared to the nominal CAD model to evaluate profile deviation. Obviously, the accuracy of numerical simulation is one of the most important aspects of a virtual inspection process. The deformation of non-rigid parts must be simulated accurately by finite element analysis which requires good material models and an appropriate characterization method for assessing material parameters associated with these models. For a non-rigid composite part, this work becomes highly challenging because of its complicated anisotropic nonlinear behavior. Thin orthotropic materials, such as fiber reinforced composites, can be described by a lamina constitution with four independent in-plane elastic parameters (longitudinal Young's modulus E_1, transverse Young's modulus E_2, in-plane shear modulus G_{12} and Poisson's ratio λ_{12}) [6-8]. However, during its assembly process, a non-rigid part undergoes large deformation, which makes that material constitutive properties change considerably. As a consequence, this model is no longer valid for assembly processes. Instead, hyperelasticity provides a framework for modelling large anisotropic deformation. According to the Lagrangian description, the constitutive properties of the material (stiffness) varies with the gradient of deformation and the anisotropic effect is characterized by the fiber's reorientation. This framework was successfully used in characterizing the behavior of fiber-reinforced composites. Pham et al. [9], Aimene et al. [10], Peng et al. [11] and Gong et al. [12] proposed hyperelastic constitutive material models and demonstrated their suitability for modelling large anisotropic deformation of fiber reinforced composites in manufacturing processes. Therefore, a hyperelastic constitutive model in the form of a strain energy function could be an appropriate approach to characterize the anisotropic behavior of flexible fiber-reinforced thermoplastic composites (FRTPC) during assembly processes.

Even if a very well-suited constitutive model is chosen, determining accurate material parameters is also one of the most important prerequisites in order to obtain reliable results from an assembly process simulation. Therefore, parameters of the constitutive model considered must be estimated by the most appropriate method. Simulation-based inverse characterization is a powerful and efficient tool to characterize the mechanical behavior of materials. This procedure is based on an optimization process that minimizes a multi-objective function that expresses discrepancies between experimental data of characterization tests and computed responses for these tests. Here, the computed responses are used as "function evaluation" and the material parameters employed in the numerical model are the variables to be determined in this optimization process. Over the past decades, a number of researchers used the inverse procedure to get the constitutive material behaviors from standard tests such as tensile tests, compression tests, bending tests, torsion tests, etc. [13-18]. However, the deformation fields generated from the standard tests in many cases cannot represent the complex deformation fields of some particular applications. In a previous study [19], the bending properties of multi-layered carbon fiber reinforced polyphenylene sulphide (CF/PPS) were obtained from three-point bending tests, but results showed that this approach needs to be improved to better characterize the behavior of non-rigid composite parts during the assembly process. To overcome this problem, non-standard experiments were developed by some researchers to be able to more accurately capture real deformation behaviors. Wang et al. [20] proposed an inverse method to determine elastic constants using a circular aluminum disk. Pagnotta [21] identified the elastic properties of materials from displacements of a thin, simply supported isotropic square plate. Bruno et al. [6] presented a method for identifying the elastic properties of aluminum and unidirectional Graphite/PEEK laminate from measurements of the displacements of plates under loading configurations. It can be seen that the selection of a test type greatly affects the accuracy of characterization. During assembly, the complexity of a non-rigid composite part behavior cannot be well characterized using a single experimental test. Obviously, the combination of results obtained from both standard and non-standard tests could lead to a more realistic description of material behavior.

In this study, in order to characterize the large bending behavior of multi-layered CF/PPS during the virtual assembly process, an inverse multi-objective optimization process combining standard and specific non-standard tests was developed. Four-layer CF/PPS sheet specimens were used for characterization. Three-point bending tests with two different stacking sequences $\left[0,90\right]_4$ and $\left[\pm 45\right]_4$ were performed as the standard method. Flexural loading tests with a large multi-layer composite sheet in different support configurations were carried out as non-standard tests. These non-standard tests were chosen because the deformation state in these tests is close to that in the assembly process. Therefore, the characterized material properties obtained from the combination of experimental data from the three-point bending test and flexural loading tests is more appropriate to represent the behavior of non-rigid composite parts during the assembly process. For the optimization procedure, numerical simulations were performed using an orthotropic hyperelastic shell formulation, which is available in ABAQUS. In this work, the anisotropic hyperelastic material model developed by Vu et al. [19] was used and implemented in ABAQUS as a user-defined material model (UMAT). The material parameters obtained from the inverse characterization procedure were validated for the case of an eight-layered CF/PPS material.

2. Experimental work

In this study, the thermoplastic composite used for the experimental works was a pre-consolidated plate of 4 layers of CF/PPS commercialized by Royal Tencate Corp. In each layer, a polyphenylene sulphide (PPS) matrix was reinforced by two orthogonal families of carbon fiber (CF). The fiber volume fraction (V_f) was of 50%. The total thickness of the four-layer laminate was approximately 1.24 mm (0.31 mm / layer).

2.1 Three-point bending test

Specimens with two different stacking sequences $[0,90]_4$ and $[\pm 45]_4$ with dimensions 300 mm × 34 mm × 1.24 mm were used for the three-point bending test. The tests were performed on the MTS testing machine. Table 1 shows the test parameters. Each specimen (5 pieces for each stacking sequence) was supported on two rollers and loaded in its center with displacement control (Figure 2). The applied force and the displacement at the center of the specimen were then recorded.

Figure 2. (a) Test specimens and (b) three point bending test using the MTS machine.

Table 1. Test parameters

Parameters	Value
Specimen dimensions	300 mm × 34 mm × 1.24 mm
Support span	140 mm
Velocity	4 mm/min
Max displacement at center of support span	20 mm
Radius of loading noses and supports	25 mm

2.2 Flexural loading test

Figure 3 shows a schematic of the flexural loading test used. A plate with dimensions 930 mm × 890 mm was supported by a system of four rigid spherical-head supports. Two different configurations of support systems were used in this test. This plate then underwent bending deformation imposed by a 3.63 kg ball applied at its center point. Table 2 summarizes experimental parameters.

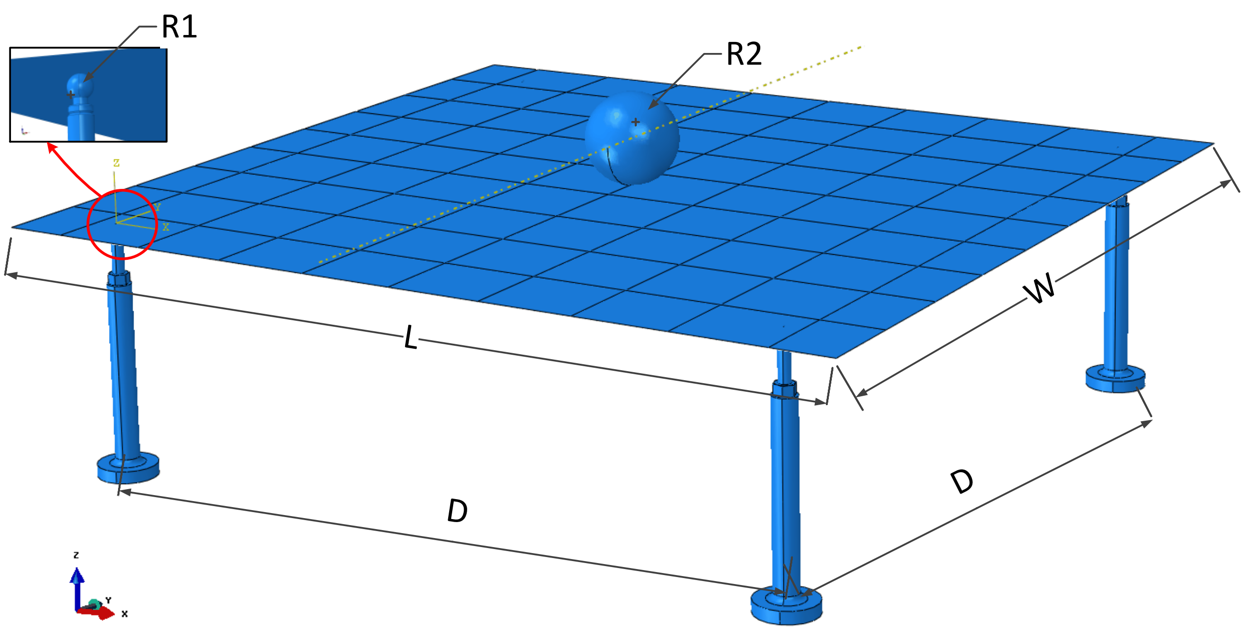

Figure 3. Flexural loading test schematic

Table 2. Experimental parameters

Composite plate	
Material	CF/PPS
Stacking sequence	$[0,90]_4$
Plate dimensions	L= 930 mm, W = 890 mm
Support system	
Radius of sphere-head supports	R_1 = 6.35 mm
Distance between supports	Configuration 1: D = 762 mm Configuration 2: D = 660.4 mm
Steel ball	
Radius of steel ball	R_2 = 49.5 mm
Weight of steel ball	3.63 kg

By using a Creaform HandyPROBE device, the displacement of the plate was measured at 110 points on the plate surface. Three measurements were performed for each support configuration to get average values. The HandyPROBE device consists of a tracking system equipped with a C-track and a handheld probe as shown in Figure 4. The triangulation obtained from two video cameras on the C-track device and the retroreflective target of the handheld probe were used to calculate the coordinates of each point.

The accuracy of the measurement is limited by uncertainty of the support system as well as the measurement process. In this work, uncertainty of the support system is approximately ±0.03 mm and ±0.02 mm for Configuration 1 and Configuration 2, while uncertainty of the measurement process is up to ±0.2 mm.

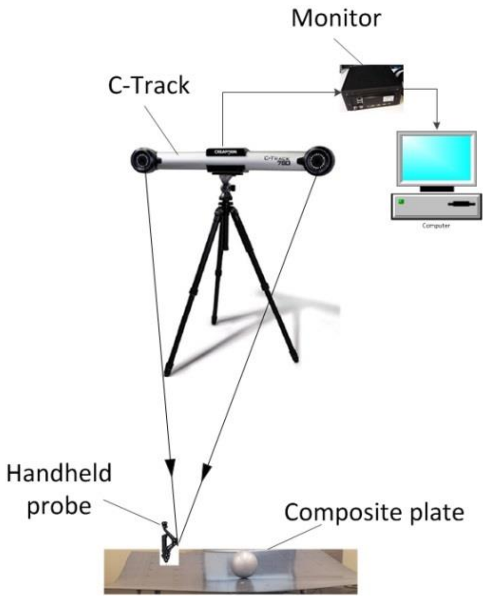

147

148 *Figure* 4. *Experimental apparatus*

149 **3. Modelling**

150 **3.1 Material model**

151 The hyperelasticity modeling concept is based on the existence of a strain energy function using
152 the Lagrangian variables, which are appropriate for the description of large deformations. The
153 mechanical behavior of a thermoplastic reinforced by two families of fiber can be represented by a
154 strain energy function of the right Cauchy-Green deformation tensor $\mathbf{C}=\mathbf{F}^{\mathrm{T}}\mathbf{F}$ and the initial fiber
155 directional unit vectors $\mathbf{a}_0$ and $\mathbf{g}_0$:

156
$$\Psi=\Psi\left(\mathbf{C},\mathbf{a}_0,\mathbf{g}_0\right) \tag{1}$$

157

158 where $\mathbf{F}=\partial\mathbf{x}/\partial\mathbf{X}$ is the deformation gradient. $\mathbf{X}$ represents the position vector of each point of the
159 solid body in the reference configuration, and $\mathbf{x}$ represents the position vector of the corresponding
160 point in the current configuration. For an orthotropic hyperelastic model, the initial directions of the
161 two fibers are orthogonal, i.e. $\mathbf{a}_0\perp\mathbf{g}_0$ and the strain energy function in Equation (1) can be written
162 in terms of invariants of $\mathbf{C}$ as:

163
$$\Psi=\Psi\left(I_1,I_2,I_3,I_4,I_6\right) \tag{2}$$

where $I_1 = \mathrm{tr}(\mathbf{C}), I_2 = \frac{1}{2}\left[\mathrm{tr}(\mathbf{C})^2 - \mathrm{tr}(\mathbf{C}^2)\right], I_3 = \det(\mathbf{C}), I_4 = \mathbf{a}_0.\mathbf{C}\mathbf{a}_0 = \lambda_{\mathbf{a}}^2,\ I_6 = \mathbf{g}_0.\mathbf{C}\mathbf{g}_0 = \lambda_{\mathbf{g}}^2$. Here, $\lambda_{\mathbf{a}}^2$ and $\lambda_{\mathbf{g}}^2$ are the square of the stretching of fibers along their initial directions $\mathbf{a}_0$ and $\mathbf{g}_0$.

The second Piola-Kirchhoff stress tensor is derived directly from the hyperelastic strain energy function and given by:

$$\mathbf{S} = 2\frac{\partial \Psi}{\partial \mathbf{C}} = 2\left(\omega_1 \frac{\partial I_1}{\partial \mathbf{C}} + \omega_2 \frac{\partial I_2}{\partial \mathbf{C}} + \omega_4 \frac{\partial I_4}{\partial \mathbf{C}} + \omega_6 \frac{\partial I_6}{\partial \mathbf{C}}\right) \tag{3}$$

where $\omega_1 = \frac{\partial \Psi}{\partial I_1}$, $\omega_2 = \frac{\partial \Psi}{\partial I_2}$, $\omega_4 = \frac{\partial \Psi}{\partial I_4}$, $\omega_6 = \frac{\partial \Psi}{\partial I_6}$.

The Cauchy stress tensor can be simply obtained by:

$$\boldsymbol{\sigma} = \frac{1}{\sqrt{\mathrm{I}_3}}\mathbf{F}\mathbf{S}\mathbf{F}^{\mathrm{T}}. \tag{4}$$

The mechanical response of CF/PPS material used in this study is represented by an orthotropic incompressible hyperelastic model proposed by Vu et al. [19]. Its strain energy function has the following form:

$$\Psi = M_1(I_1 - 3) + M_2(I_2 - 3) + M_3(I_1 - 3)(I_2 - 3) + k_1\left[\mathrm{e}^{k_2(I_4-1)^2} - 1\right] + k_3\left[\mathrm{e}^{k_4(I_6-1)^2} - 1\right] - \frac{1}{2}p(I_3 - 1) \tag{5}$$

where M_1, M_2, M_3, k_1, k_2, k_3, k_4 are the material parameters. Please refer to reference [19] for more details.

3.2 Computational experiment

The numerical simulations corresponding to the three-point bending test and flexural loading test presented in the previous section were performed using the commercial FE package Abaqus/Standard. Four-node shell elements (S4R) with a four layer composite section were used to model the specimens. Each layer behaves like an orthotropic material characterized by the constitutive model of Equation (5). A frictionless contact between the support system and the specimen was defined for both tests. For the flexural loading test, a 35.59 N concentrated force, which is equivalent to the weight of the steel ball, is set on the center point of the plate. The computational models for the three-point bending test and flexural loading test are depicted in Figure 5.

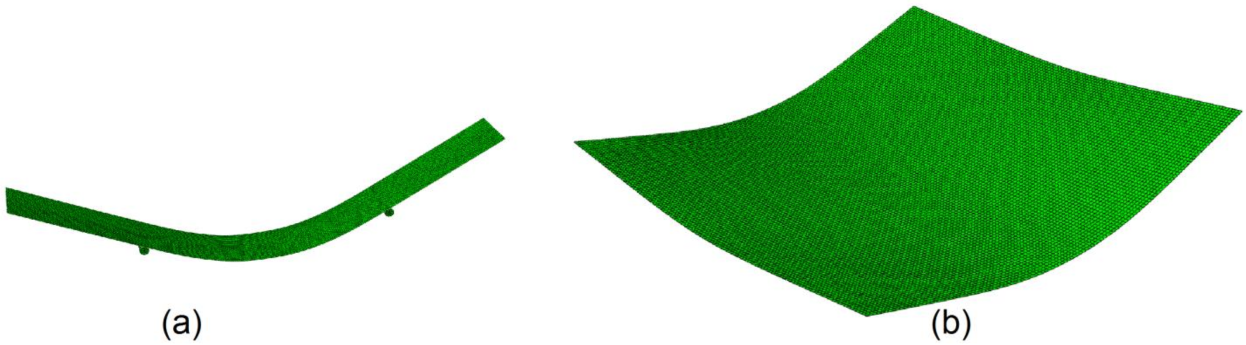

Figure 5. Computational models: (a) Three-point bending test, (b) Flexural loading test

4. Identification of constant material parameters

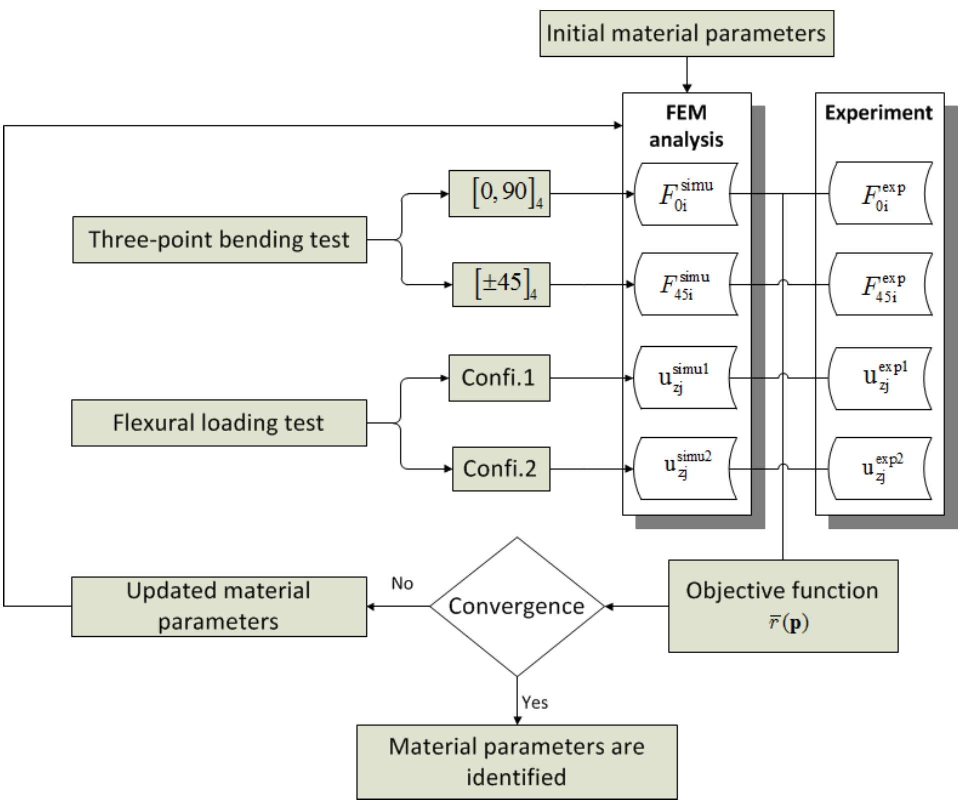

Figure 6. Inverse characterization flowchart

The material parameters M_1, M_2, M_3, k_1, k_2, k_3, k_4 of the strain energy function in Equation (5) for multi-layered carbon fiber reinforced material are identified by minimizing objective functions that represent discrepancy between experimental test data and numerical simulation results. The updated material parameters were performed with the Global Response Surface Method for multi-objective optimization. As presented in (equation 6?) Figure 6, the difference of loads between experimental data and numerical results was taken into account for building the objective function associated with the three-point bending test while vertical plate displacements were used to build the objective function associated with the flexural loading test. These objective functions are as follows:

$$\overline{r}_{\mathrm{b}}(\mathbf{p}) = \sqrt{\frac{1}{2\mathrm{N_b}}\left\{\sum_{\mathrm{i=1}}^{\mathrm{N_b}}\left(\frac{F_{0\mathrm{i}}^{\mathrm{exp}} - F_{0\mathrm{i}}^{\mathrm{simu}}(\mathbf{p})}{F_{0\mathrm{max}}^{\mathrm{exp}}}\right)^2 + \sum_{\mathrm{i=1}}^{\mathrm{N_b}}\left(\frac{F_{45\mathrm{i}}^{\mathrm{exp}} - F_{45\mathrm{i}}^{\mathrm{simu}}(\mathbf{p})}{F_{45\mathrm{max}}^{\mathrm{exp}}}\right)^2\right\}} \tag{6}$$

$$\overline{r}_{\mathrm{f}}(\mathbf{p}) = \sqrt{\frac{1}{2\mathrm{N_f}}\left\{\sum_{\mathrm{j=1}}^{\mathrm{N_f}}\left(\frac{\mathrm{u_{zj}^{exp1}} - \mathrm{u_{zj}^{simu1}}(\mathbf{p})}{\max(\mathrm{u_{zj}^{exp1}})}\right)^2 + \sum_{\mathrm{j=1}}^{\mathrm{N_f}}\left(\frac{\mathrm{u_{zj}^{exp2}} - \mathrm{u_{zj}^{simu2}}(\mathbf{p})}{\max(\mathrm{u_{zj}^{exp2}})}\right)^2\right\}} \tag{7}$$

Herein, $\mathbf{p}$ is the list of unknown parameters. The relative error values $\overline{r}_{\mathrm{b}}(\mathbf{p})$ and $\overline{r}_{\mathrm{f}}(\mathbf{p})$ represent the objective functions of the three-point bending test and flexural loading test respectively. $\mathrm{N_b}$ is the number of displacement steps at which loads were measured in the three-point bending test. $F_{0\mathrm{i}}^{\mathrm{exp}}$ and $F_{0\mathrm{i}}^{\mathrm{simu}}$ represent the experimental and computed loads respectively at step i for the stacking sequence $[0,90]_4$. $F_{45\mathrm{i}}^{\mathrm{exp}}$ and $F_{45\mathrm{i}}^{\mathrm{simu}}$ represent the experimental and computed loads respectively at step i for the stacking sequence $[\pm 45]_4$. $\mathrm{N_f}$ is the number of measured points on the plate surface in the flexural loading test. $\mathrm{u_{zj}^{exp1}}$ and $\mathrm{u_{zj}^{simu1}}$ denote the experimental and numerical vertical displacements at point j for Configuration 1. $\mathrm{u_{zj}^{exp2}}$ and $\mathrm{u_{zj}^{simu2}}$ denote the experimental and numerical vertical displacements at point j for Configuration 2.

Convergence criterion is set to be reached when the updated parameter values are (difference ?) inferior to 0.5% of actual parameter values. The iterative process ended after 11 steps of the updating process. Table 3 shows the converged parameter values.

Table 3. Optimized parameter values

M_1 (MPa)	M_2 (MPa)	M_3 (MPa)	k_1 (MPa)	k_2	k_3 (MPa)	k_4
703.3	915.0	512.0	1131.0	46.2	1131.0	46.2

Good agreement was found between experimental and computed loads associated with the three-point bending test versus displacement for the optimized parameters set (Figure 7). With the small value of relative errors $\bar{r}_{\mathrm{b}}(\mathbf{p}) = 0.0173$, it turned out that the inverse procedure leads to a good fit between experimental and numerical loads.

Figure 8 and Figure 9 show the residual difference between measured and calculated vertical displacement of composite plate for flexural loading tests. The average differences between experimental and numerical results were found to be 1.53 mm for Configuration 1, and 0.88 mm for Configuration 2. The relative error $\bar{r}_{\mathrm{f}}(\mathbf{p})$ is 0.056. It demonstrated that a good match of the calculated and the measured vertical displacement was achieved as well for the flexural loading test.

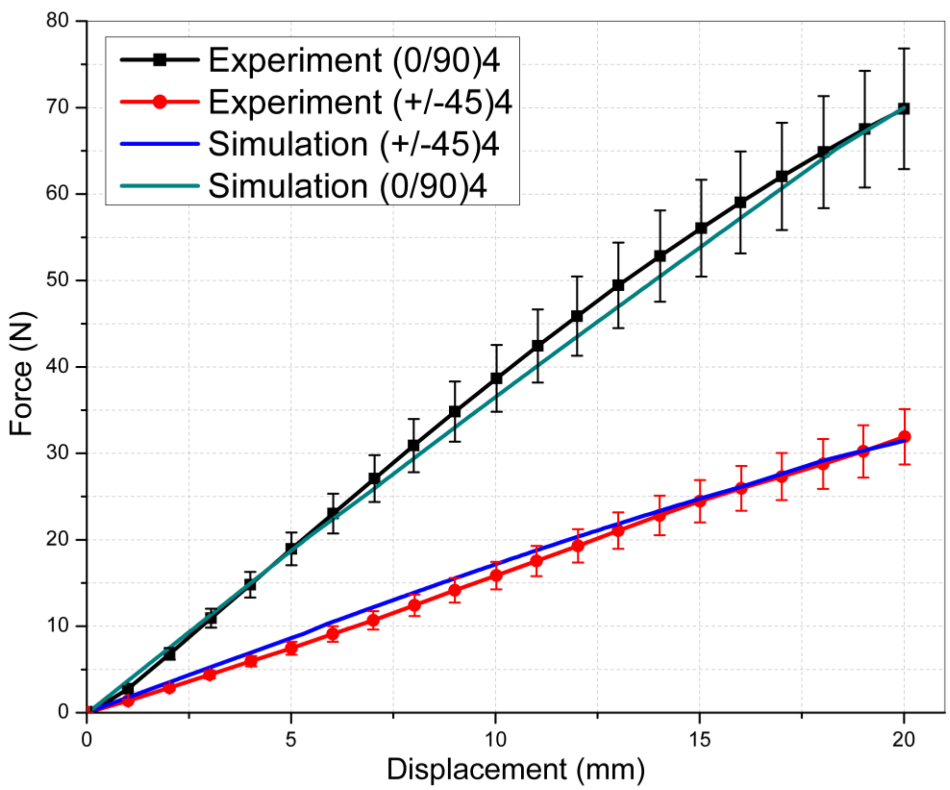

Figure 7 Comparison between numerical results and experimental data for three-point bending test

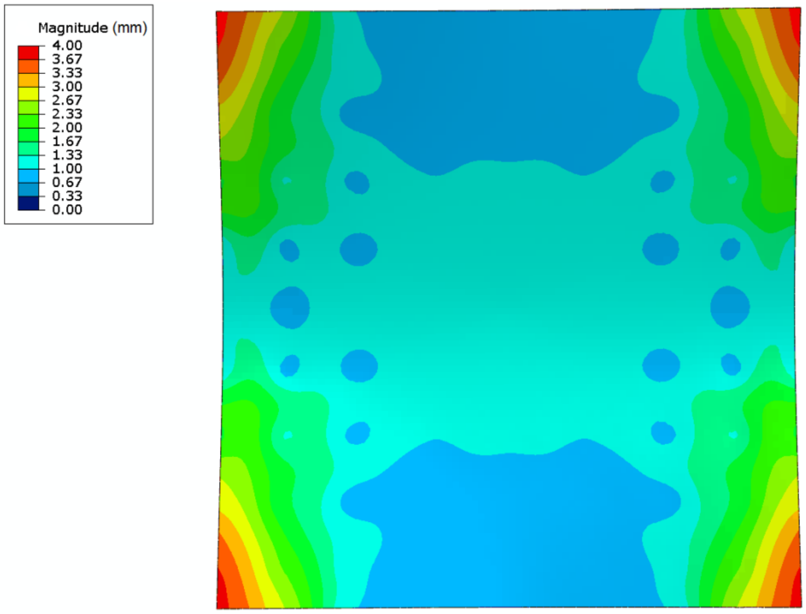

Figure 8. Residual difference between measured and calculated vertical displacement for Configuration 1

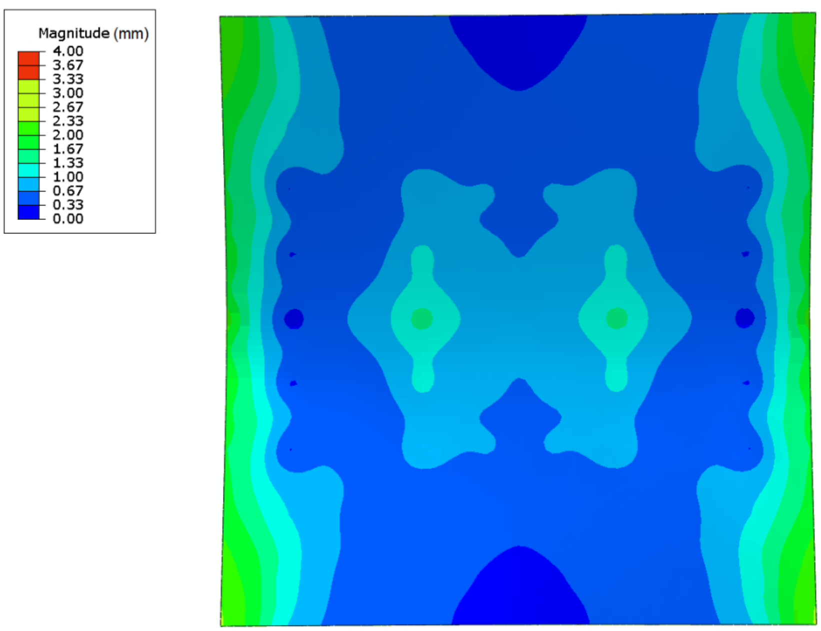

Figure 9. Residual difference between measured and calculated vertical displacement for Configuration 2

5. Validation of material model

In this study, the material used for validating the material model is a consolidated plate of eight layers of CF/PPS with 2.48 mm thickness (0.31 mm/layer). The stacking sequence of plates is $\left[(0,90)/\pm45/\pm45/(0,90)\right]_s$. The flexural loading test for this plate of eight-layer laminate was performed using the same experimental set up as that used for the four-layer laminate in the previous section. Dimensions of the plate were 1200 mm x 1200 mm x 2.48 mm. Two validation cases with two different configurations were performed in this work (see Figure 10). Vertical displacement was measured at 169 points on the plate surface.

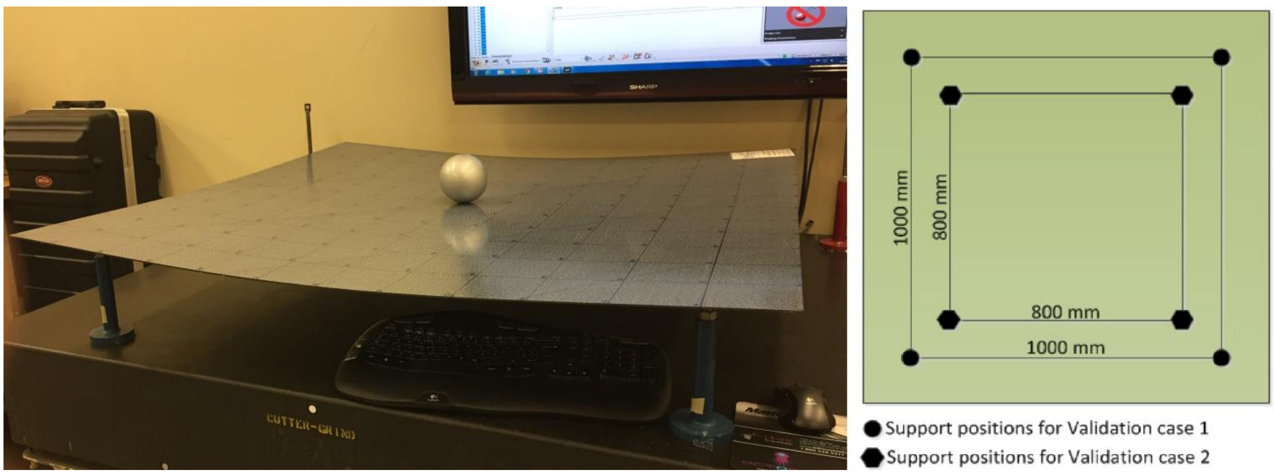

Figure 10. Validation test

A FEA simulation procedure with Abaqus was applied to compute vertical plate displacements. The material parameters obtained from the inverse characterization procedure were used to simulate the deformation of this composite plate.

Figure 11 and Figure 12 show the residual difference between measured and calculated vertical displacement of the composite plate for these two validation cases. The average difference between experimental and numerical results was found to be 1.42 mm and 0.55 mm respectively for validation case 1 and case 2. Small relative errors obtained ($\bar{r}_1$ = 0.0582 for validation case 1 and $\bar{r}_2$ = 0.0283 for validation case 2 demonstrated that the material model used here is appropriate for assessing the mechanical behavior of this multilayered composite and that the identification procedure developed in this paper is suitable for the characterization of this composite material.

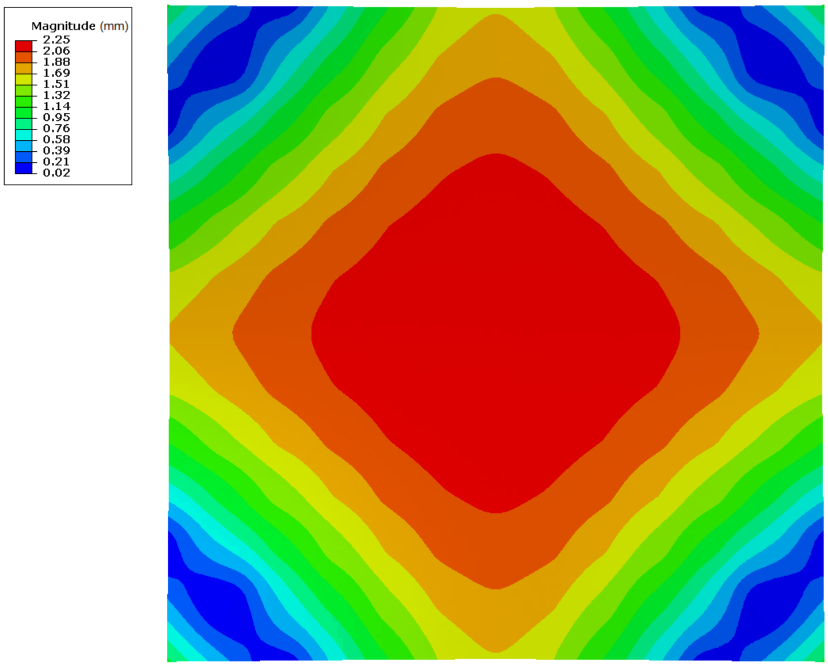

Figure 11. Residual difference between measured and calculated vertical displacement for Validation case 1

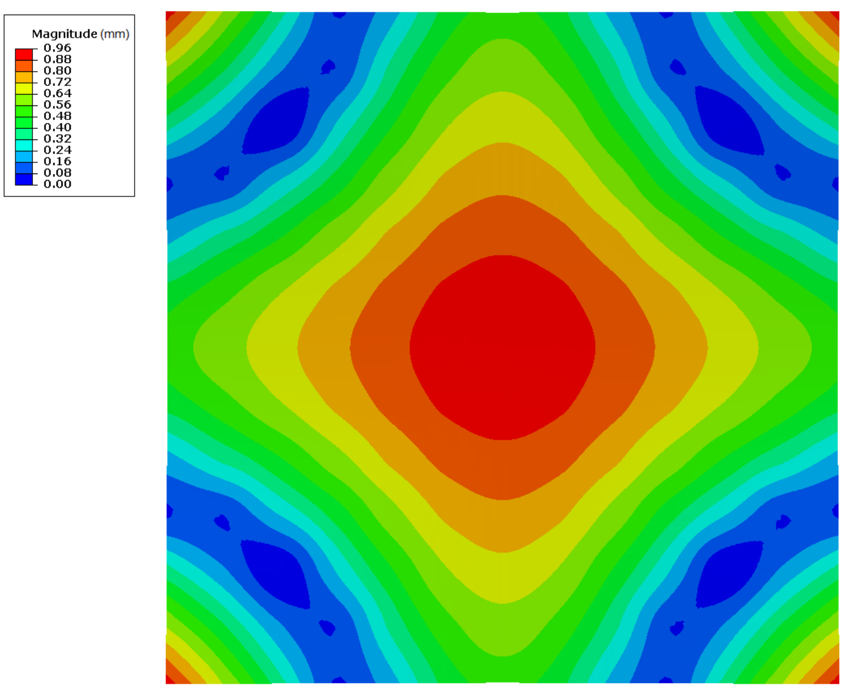

Figure 12 Residual difference between measured and calculated vertical displacement for Validation case 2

6. Conclusion

In this paper, an inverse procedure was developed for characterizing the large bending deformation behavior of four layers of CF/PPS material. A three-point bending test with two different stacking sequences and a flexural loading test with two different configurations for boundary conditions were performed to study the mechanical responses. FEA modelling was performed using the Abaqus/Standard commercial FE package based on an orthotropic hyperelastic model for finite strain shell elements. Material parameters associated with this hyperelastic model were identified by minimizing discrepancy between experimental and numerical data. The material model parameters obtained from the inverse characterization were validated for the case of an eight-layer CF/PPS material. Results showed that the proposed method is appropriate for characterizing the behavior of multi-layered composites in large deformation. The method presented in this paper can be applied to characterize and simulate the large anisotropic deformation behavior of non-rigid composite parts during the virtual assembly process.

Acknowledgments

The authors would like to thank the National Sciences and Engineering Research Council (NSERC) and our industrial partner: Bombardier Aerospace, Consortium for Aerospace Research and Innovation in Québec (CRIAQ) for their support and financial contribution.

References

1. Aidibe, A., Tahan, A.: Adapting the coherent point drift algorithm to the fixtureless dimensional inspection of compliant parts. The International Journal of Advanced Manufacturing Technology 79(5), 831-841 (2015). doi:10.1007/s00170-015-6832-9.
2. Aidibe, A., Tahan, A.S., Abenhaim, G.N.: Distinguishing profile deviations from a part's deformation using the maximum normed residual test. Wseas Transaction on Applied and Theorical Mechanics 7(1), 18-28 (2012).
3. Abenhaim, G.N., Tahan, A.S., Desrochers, A., Maranzana, R.: A Novel Approach for the Inspection of Flexible Parts Without the Use of Special Fixtures. Journal of Manufacturing Science and Engineering 133(1), 011009-011009-011011 (2011). doi:10.1115/1.4003335.
4. Gentilini I and Shimada K. Predicting and evaluating the post-assembly shape of thin-walled components via 3D laser digitization and FEA simulation of the assembly process. Computer-Aided Design 2011; 43: 316-328. DOI: 10.1016/j.cad.2010.11.004.
5. Weckenmann, A., Weickmann, J.: Optical inspection of formed sheet metal parts applying fringe projection systems and virtual fixation. Metrology and Measurement Systems Vol. 13, nr 4, 321-334 (2006).
6. Bruno L, Felice G, Pagnotta L, et al. Elastic characterization of orthotropic plates of any shape via static testing. International Journal of Solids and Structures 2008; 45: 908-920. DOI: 10.1016/j.ijsolstr.2007.09.017.
7. Genovese K, Lamberti L and Pappalettere C. A new hybrid technique for in-plane characterization of orthotropic materials. Experimental Mechanics 2004; 44: 584-592. DOI: 10.1007/BF02428248.
8. Wang WT and Kam TY. Material characterization of laminated composite plates via static testing. Composite Structures 2000; 50: 347-352. DOI: https://doi.org/10.1016/S0263-8223(00)00112-4.
9. Pham X-T, Bates P and Chesney A. Modeling of Thermoforming of Low-density Glass Mat Thermoplastic. J. Reinf. Plast. Compos. 2005; 24: 287-298.
10. Aimène Y, Vidal-Sallé E, Hagège B, et al. A Hyperelastic Approach for Composite Reinforcement Large Deformation Analysis. Journal of Composite Materials 2009; 44: 5-26.

11. Peng X, Guo Z, Du T, et al. A simple anisotropic hyperelastic constitutive model for textile fabrics with application to forming simulation. Composites Part B: Engineering 2013; 52: 275-281.

12. Gong Y, Peng X, Yao Y, Guo Z. An anisotropic hyperelastic constitutive model for thermoplastic woven composite prepregs. Compos. Sci. Technol. 2016;128:17-24.

13. Kajberg J and Lindkvist G. Characterisation of materials subjected to large strains by inverse modelling based on in-plane displacement fields. International Journal of Solids and Structures 2004; 41: 3439-3459. DOI: https://doi.org/10.1016/j.ijsolstr.2004.02.021.

14. Lecompte D, Smits A, Sol H, et al. Mixed numerical–experimental technique for orthotropic parameter identification using biaxial tensile tests on cruciform specimens. International Journal of Solids and Structures 2007; 44: 1643-1656. DOI: https://doi.org/10.1016/j.ijsolstr.2006.06.050.

15. Belhabib S, Haddadi H, Gaspérini M, et al. Heterogeneous tensile test on elastoplastic metallic sheets: Comparison between FEM simulations and full-field strain measurements. International Journal of Mechanical Sciences 2008; 50: 14-21. DOI: https://doi.org/10.1016/j.ijmecsci.2007.05.009.

16. Guélon T, Toussaint E, Le Cam JB, et al. A new characterisation method for rubber. Polymer Testing 2009; 28: 715-723. DOI: https://doi.org/10.1016/j.polymertesting.2009.06.001.

17. Liu H, Shen Y, Yang S, et al. A comprehensive solution to miniaturized tensile testing: Specimen geometry optimization and extraction of constitutive behaviors using inverse FEM procedure. Fusion Engineering and Design 2017; 121: 188-197. DOI: 10.1016/j.fusengdes.2017.07.016.

18. Cooreman S, Lecompte D, Sol H, et al. Identification of Mechanical Material Behavior Through Inverse Modeling and DIC. Experimental Mechanics 2007; 48: 421-433. DOI: 10.1007/s11340-007-9094-0.

19. Vu N-H, Pham X-T, François V, et al. Characterization of multilayered carbon-fiber–reinforced thermoplastic composites for assembly process. Journal of Thermoplastic Composite Materials 2018: 0892705718772878. DOI: 10.1177/0892705718772878.

20. Wang Z, Cárdenas-García JF and Han B. Inverse method to determine elastic constants using a circular disk and moiré interferometry. Experimental Mechanics 2005; 45: 27-34. DOI: 10.1007/BF02428987.

21. Pagnotta L. Determining elastic constants of materials with interferometric techniques. Inverse Problems in Science and Engineering 2006; 14: 801-818. DOI: 10.1080/17415970600838806.